Marie Skłodowska-Curie (MSCA) – Innovative Training Networks (ITN)
H2020-MSCA-ITN European Training Networks

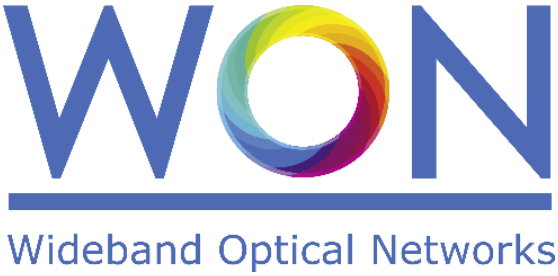

Wideband Optical Networks [WON]

Grant agreement ID: 814276

WP2 – Digital signal processing and system modelling

Deliverable D2.2 The generalized Gaussian noise model (GGN) for the entire single mode spectrum

This project has received funding from the European Union's Horizon 2020 research and innovation programme under the Marie Skłodowska-Curie grant agreement 814276.

Document Details

Work Package	WP2 – Digital signal processing and system modelling
Deliverable number	D2.2
Deliverable Title	The generalized Gaussian noise model (GGN) for the entire single mode spectrum
Lead Beneficiary:	POLITO
Deliverable due date:	31 August 2021
Actual delivery date:	5 May 2022
Dissemination level:	Public

Project Details

Project Acronym	WON
Project Title	Wideband Optical Networks
Call Identifier	H2020-MSCA-2018 Innovative Training Networks
Coordinated by	Aston University, UK
Start of the Project	1 January 2019
Project Duration	48 months
WON website:	https://won.astonphotonics.uk/
CORDIS Link	https://cordis.europa.eu/project/rcn/218205/en

WON Consortium and Acronyms

Consortium member	**Legal Entity Short Name**
Aston University	Aston
Danmarks Tekniske Universitet	DTU
VPIphotonics GmbH	VPI
Infinera Portugal	INF PT
Fraunhofer HHI	HHI
Politecnico di Torino	POLITO
Technische Universiteit Eidhoven	TUE
Universiteit Gent	UG
Keysight Technologies	Keysight
Finisar Germany GmnH	Finisar
Orange SA	Orange
Technische Universitaet Berlin	TUB
Instituto Superior Tecnico, University of Lisboa	IST

Abbreviations

ASE:	Amplified spontaneous emission
AWG:	Additive and white Gaussian
CUT:	Channel under test
EDFA:	Erbium-Doped Fibre Amplifiers
FWM:	Four-wave mixing
G:	Gain
GGN:	Generalized Gaussian Noise
GN:	Gaussian Noise
GSNR:	Generalized signal-to-noise ratio
LP:	Lightpath
NF:	Noise-figure
NLI:	Nonlinear interference
OLC:	Optical line controller
OLS:	Optical line system
OSNR:	Optical signal-to-noise ratio
PSD:	Power spectral density
PUMP:	Interfering channel
QoT:	Quality of transmission
SNR_{NL}:	Nonlinear signal-to-noise ratio
SPM:	Self-phase modulation
SRS:	Stimulated Raman scattering
SSFM:	Split-step Fourier method
SSMF:	Standard single-mode fibre
TDFA:	Thulium-Doped Fibre Amplifiers
XPM:	Cross-phase modulation

CONTENTS

LIST OF FIGURES

EXECUTIVE SUMMARY

The present scientific deliverable “The generalized Gaussian noise model (GGN) for the entire single mode spectrum” is part of the Work Package 2 “ Digital signal processing and system modelling” of the European Training Network “ Wideband Optical Networks (WON)” funded under the Horizon 2020 Marie Skłodowska-Curie scheme Grant Agreement 814276.

This document provides details on the state-of-art of fibre transmission modelling, focused on the application of the generalized Gaussian Noise model applied to a multi-band transmission scenario. The main topics carried out and presented in this text are: (i) description of the multi-band transmission abstraction and the disaggregated approach used to compute the quality of transmission; (ii) detailing of fibre and amplifier parameters in order to properly model the multi-band transmission; (iii) description and results of the GGN model for wide bandwidth.

1. Overview of multi-band optical line systems and disaggregated optical networking

The current increasing in data traffic led by imminent 5G services implementation, cloud computing and data centres interconnections, will stress the demand required from optical networks. For this reason, solutions aiming the increasing of overall network capacity are being investigated in order to cope with that demand. The proposed multi-band transmission [1] is the most viable solution for short-term application, as it uses the already deployed fibre infrastructure of current optical networks. This approach aims the transmission over the entire low-loss fibre spectrum (around 50 THz for standard single-mode fibres – SSMF) split in 5 bands (L- to O-bands), as shown in Figure 1. Nowadays those systems operate mainly using C-band only, or C+L transmission systems.

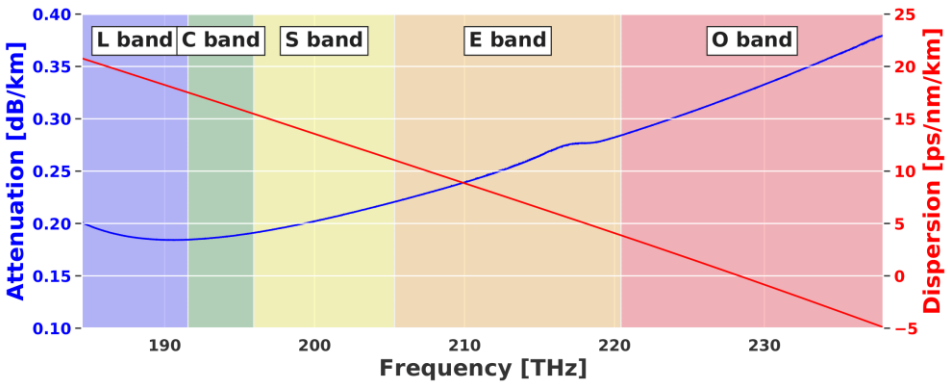

Figure 1: Attenuation and dispersion profiles for the entire low-loss SSMF spectrum.

In this scenario, each amplification site within an optical line system (OLS), which compose the entire optical network, is made of several amplifiers, each one responsible for the amplification of a specific part of the spectrum. Figure 2 illustrate a network and an OLS with three bands (L, C and S). Another part of the abstraction is the optical line controller (OLC) which is responsible to control each amplifier working point, based on a quality of transmission (QoT) evaluation. In several works [2] [3] this evaluation is performed using the open-source GNPy tool [4], the same used in this work.

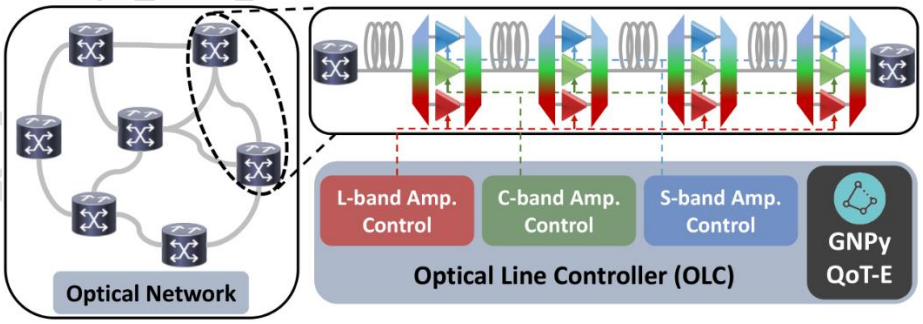

Figure 2: Optical network and optical line system abstraction for a multi-band transmission scenario.

The QoT is quantified by the generalized signal-to-noise ratio (GSNR) for each transmitted channel (lightpath – LP), assuming it as an additive and white Gaussian (AWG) noise, which can be expressed as:

$$GSNR(f) = (OSNR(f)^{-1} + SNR_{NL}(f)^{-1})^{-1} = \left(\left(\frac{P_{ASE}(f)}{P_{in}(f)}\right)^{-1} + \left(\frac{P_{NLI}(f)}{P_{in}(f)}\right)^{-1}\right)^{-1}$$

where the $OSNR$ is the optical signal-to-noise ratio including all the linear contributions (amplified spontaneous emission (ASE) noise power - P_{ASE}) and the SNR_{NL} is the nonlinear signal-to-noise ratio, including all the nonlinear impairments generated during the fibre propagation [5] (nonlinear interference – NLI, depending on the NLI power - P_{NLI}). Each $GSNR$ is computed for every transmitted channel in frequency f for each span s traversed the LP l by the channel, with the total GSNR given by:

$$GNSR_{total}(f) = \frac{1}{\sum_{s \in l}(GSNR_s(f))^{-1}}$$

In order to use the aforementioned QoT quantification, regarding the NLI used to compute the SNR_{NL}, a disaggregated approach is desirable. This approach includes several benefits: Firstly, vendors may not willing to disclose essential spectral or device information due to private reasons. Secondly, shared network infrastructure can present alien LP, which are channels operated by a third-party vendor that may have unknow source/destination nodes [6]. If channels are treated from a disaggregated standpoint, these issues are lessened for the NLI modelling. Section 3 describes in detail the QoT computation using the disaggregated approach, highlighting the characteristics for multi-band transmission.

2. Multi-band physical layer parameters

The first physical layer parameter needed in order to proper model a multi-band transmission is the fibre loss coefficient. Due to the fibre composition and manufacturing process [7], the loss coefficient (dB/km) depends on the wavelength of the propagating channel. In [8] is presented a loss coefficient model with respect to each phenomenological factor, expressed as:

$$\alpha(\lambda) \simeq \alpha_S(\lambda) + \alpha_{UV}(\lambda) + \alpha_{IR}(\lambda) + \alpha_{13}(\lambda) + \alpha_{12}(\lambda) + \alpha_{POH}(\lambda)$$

represented by the Rayleigh scattering, ultraviolet, infrared, OH^- and (P)OH peak absorption contributions, respectively, in dB/km. Using the definition presented in [8], the loss coefficient profile for the entire spectrum used in a multi-band scenario can be estimated.

The second parameter required to properly model the multi-band transmission is the chromatic dispersion, which determines the broadening of an optical pulse propagating over a fibre. This phenomenon is modelled by the Taylor series expansion of the mode-propagation constant, β, with respect to the central frequency of the pulse [9]. The second derivative β_2 describes the pulse broadening. Usually, optical fibre manufacturers provide the dispersion parameter D as a function of the zero dispersion wavelength λ_0 and slope S_0:

$$D(\lambda) \approx \frac{S_0}{4}\left[\lambda - \frac{\lambda_0^4}{\lambda^3}\right]$$

With it, we can find the β_2 expressed as:

$$\beta_2(\lambda) = -\frac{\lambda^2}{2\pi c} D(\lambda)$$

where c is the speed of light in the vacuum. The dispersion slope S_0 can be used to express the third derivative β_3 as:

$$\beta_3(\lambda) = \frac{S_0 - \left(\frac{4\pi c}{\lambda^3}\right)\beta_2(\lambda)}{\left(\frac{2\pi c}{\lambda^2}\right)^2}$$

Another fibre parameter, the nonlinear coefficient γ, is responsible to weight the nonlinear contribution. It is defined as:

$$\gamma(\lambda) = \frac{2\pi}{\lambda}\frac{n_2}{A_{eff}}$$

where n_2 is the nonlinear refractive index and A_{eff} is the effective mode area. The effective area is defined as $A_{eff} = \pi w^2$, where w is the mode radius which depends upon the central pulse wavelength and the fibre geometry. In this way, also the nonlinear coefficient profile can be defined for the entire low loss spectrum.

In a WDM multi-band transmission, another effect which needs be considered is the stimulated Raman scattering (SRS) [10]. This effect results in a power transfer from higher to lower frequency channels along the fibre propagation. This power transfer is regulated by the Raman gain coefficient g based on the frequency shift $\Delta f = f_p - f_s$ between the higher (f_p) and lower (f_s) frequencies, with peak power transfer at around $\Delta f = 13$ THz, as presented in
Figure 3. Due to the power transfer resulting from the SRS effect, the NLI contribution must be computed considering this effect. Section 3 describes how this computation can be performed. The SRS power evolution for a 75 km SSMF is shown in
Figure 4, which highlights the change in power profile along the fibre transmission. Finally, to further highlight the SRS effect, Figure 5 shows the output power profile at the end of the optical fibre when input launched powers of 0.6, -0.1 and 0.8 dBm for L-, C- and S_1-bands, respectively are considered. As an example, we can see that, at the optical fibre output, the SRS effect may cause a variation of the power level in the S_1-band of around 5 dB, which stresses the need to take the SRS effect accurately into account in multi-band transmission systems. Regarding the S-band, we highlight that we made use of only part of it, in order to obtain an additional bandwidth with the same amount of C-band, which is 4.8 THz. As the total S-band has almost the double of bandwidth of the C-band, we use the notation S_1 to define the first portion of this band.

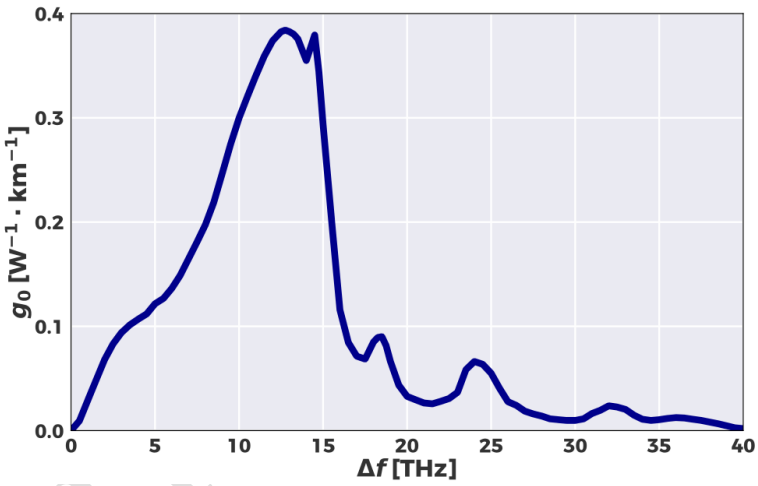

Figure 3: Experimental Raman gain coefficient curve for fused silica.

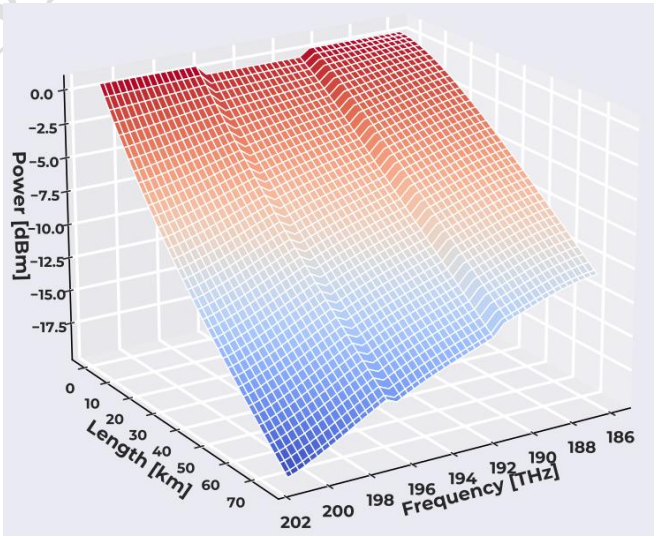

Figure 4: SRS power evolution transmitting over a 75 km SSMF.

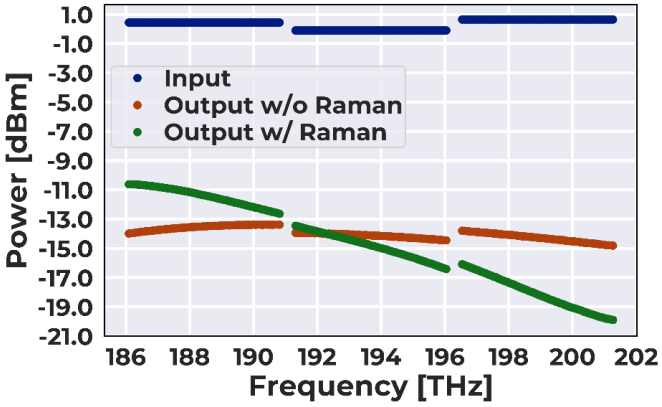

Figure 5: Input and output power profile with and without considering the SRS effect, propagating over a 75 km SSMF.

Finally, as briefly described in Section 1, an optical transmission scenario beyond the C+L bandwidth will require different amplification devices for each portion of the spectrum. In this way we can cope with the limited bandwidth and output power of the devices (optical amplifiers). Nowadays, the OLSs are amplified by Erbium-Doped Fibre Amplifiers (EDFAs) which can work in both C- and L-bands, but don't perform well for the entire fibre low loss spectrum. For other bands, such as S-band, the amplification will depend on other types of doped fibres amplifiers, such as thulium-DFA (TDFA) [11]. Other types of amplifiers are being studied for E-band, such Nd^{3+} fibre amplifier [12] and bismuth-DFA (BDFA) [13]. The two main parameters of each amplifier, required to proper model the QoT, are the gain (*G*) and noise-figure (NF), which will determine the amplified spontaneous emission (ASE) noise added to the optical signal and the total signal loss after each fiber span. These parameters will be discussed in detail in Section 3. An example of the NF of EDFA/TDFA retrieved from commercial amplifiers for C-, L- and S_1-bands, with bandwidths occupying the same amount of spectrum, are shown in Figure 6.

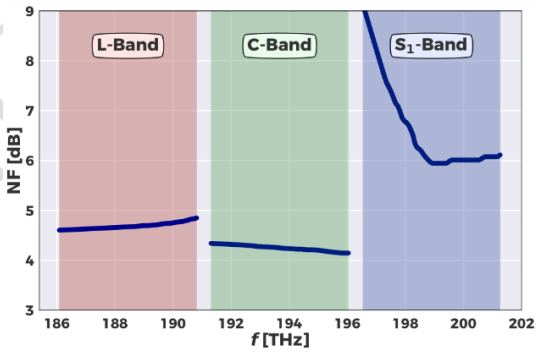

Figure 6: NF of EDFA (C- and L-bands) and TDFA (S-band) versus frequency.

Taking the amplifier characteristics for each band, is possible to compute the ASE contribution as shown in [14], where:

$$P_{ASE}(f) = h \cdot f \cdot NF(f) \cdot G(f) \cdot B_{ref}$$

where h is the Plank's constant, B_{ref} is the reference bandwidth and *NF* and *G* are the noise-figure and gain of the amplifier, respectively. With all the frequency dependent parameters properly stablished for a multi-band scenario, is possible to compute the QoT without any loss of generality.

3. Disaggregated GGN applied to multi-band

The NLI contribution can be split into three contributions: Self-phase modulation (SPM), cross-phase modulation (XPM) and four-wave mixing (FWM). According to [14], the FWM is negligible for most practical scenarios. Based on that, only the SPM, which arises from the NLI generated by a channel interfering with itself, and XPM, which arises from the NLI generated between the channel under test (CUT) and all the other interfering channels of the comb (PUMPs). Using the disaggregation hypothesis, the NLI power ($P_{NLI}(f)$) of a CUT with frequency f is defined as [15]:

$$P_{NLI}(f) = P_{NLI,0}(f) + \sum_{k\neq 0} P_{NLI,k}(f),$$

where the first term refers to the SPM and the second term refers to the XPM, which is a sum of all possible interference between the channels of the comb and the CUT.

To compute the NLI contribution in a disaggregated manner, the Gaussian Noise (GN) model [16] is usually a fast but still accurate enough and conservative model for NLI prediction in C-band only transmission systems. However, as the used spectral bandwidth increases, this model is no longer recommended as it does not consider the impact of SRS. To cope with this aspect, the generalized GN model (GGN) was proposed, aiming to assess the interplay of NLI generation with spatial and frequency power variations along the fibre [10]. The NLI power can be defined as:

$$P_{NLI}(f) = B_{ref} G_{NLI}(L_S, f)$$

where B_{ref} is the reference bandwidth and $G_{NLI}(L_S, f)$ is the power spectral density (PSD) generated by the NLI. Accordingly to Eq. 24 of [17], the NLI PSD can be expressed as:

$$G_{NLI}(L_S, f) = \frac{16}{27}\gamma^2 \rho(z,f)^2 \iint_{-\infty}^{\infty} G_{TX}(f_1) G_{TX}(f_2) G_{TX}(f_1+f_2-f) \cdot$$
$$\cdot \left[\int_0^{L_s} e^{+j\Delta\beta(f,f_1,f_2)z} \cdot \frac{\rho(z,f_1)\rho(z,f_1+f_2-f)\rho(z,f_2)}{\rho(z,f)} dz \right]^2 df_1 df_2$$

where $G_{TX}(f)$ is the PSD of a transmitted channel and $\rho(z,f)$ is the overall frequency and space dependent fibre loss profile, which considers the SRS effect. Applying this equation in a disaggregated manner, we can calculate the SPM contribution for the CUT as:

$$P_{NLI}^{SPM}(f_{CUT}) = B_{ref} \cdot W_{SPM} \cdot \gamma(f_{CUT})^2 \rho(z, f_{CUT})^2 \left(\frac{P_{CUT}}{R_{S,CUT}} \right)^3 \cdot$$
$$\cdot \iint_{-\infty}^{\infty} \left[\int_0^{L_s} e^{+j\Delta\beta(f_{CUT},f_1,f_2)z} \cdot \frac{\rho(z,f_1)\rho(z,f_1+f_2-f_{CUT})\rho(z,f_2)}{\rho(z,f_{CUT})} dz \right]^2 df_1 df_2$$

and the XPM NLI contribution for one particular PUMP channel as:

$$P_{NLI}^{XPM}(f_{CUT}) = B_{ref} \cdot W_{XPM} \cdot \gamma(f_{CUT})^2 \rho(z, f_{CUT})^2 \left(\frac{P_{CUT}}{R_{S,CUT}} \right) \left(\frac{P_{PUMP}}{R_{S,PUMP}} \right)^2 \cdot$$

$$\cdot \iint_{-\infty}^{\infty} \left[\int_{0}^{L_s} e^{+j\Delta\beta(f_{CUT},f_1,f_2)z} \cdot \frac{\rho(z,f_1)\rho(z,f_1+f_2-f_{CUT})\rho(z,f_2)}{\rho(z,f_{CUT})} dz \right]^2 df_1 df_2$$

in which the SPM and XPM weights are defined as $W_{SPM} = (1 + C_\infty)\frac{16}{27}$ and $W_{XPM} = 2 \cdot \frac{16}{27}$ coming from the statistics and the polarization, in which the coefficient C_∞ represents the asymptotic level of the the coherent accumulation of the SPM [19]. In order to validate the disaggregation assumption, the first plot of Figure 7 presents a split-step Fourier method simulation (SSFM), comparing the SNR_{NL} computed when assuming transmission in the full spectrum of 15 channels and when assuming the superposition approach (sum of SPM and XPM using pump-and-probe). In this simulation, the transmission of 15 coherent channels within a 75 GHz WDM grid, with a symbol rate of 64 Gbaud and roll-off of 0.15 shaped using a raised-cosine filter is assumed. The CUT is located at 193.9 THz (centre of the comb). Moreover, the OLS is composed of 3 different fibre types (5 spans each), with different values of dispersion, in order to simulate different scenarios that can be found in real networks. The first plot of Figure 7 shows that the assumption of the superposition presents similar values of the full spectrum simulation, with the disaggregated GGN presenting a conservative prediction for all spans. The second plot of Figure 7 shows the $\mathrm{SNR_{NL}}$, the OSNR and GSNR, comparing again the full spectrum, superposition and GGN results. For the GSNR, the full spectrum and superposition presented similar results while the GGN method shows a conservative estimation with 0.4 dB of difference after 15 spans. These results shown that the full spectrum scenario can be recovered by its superimposing contributions, validating the disaggregated approach.

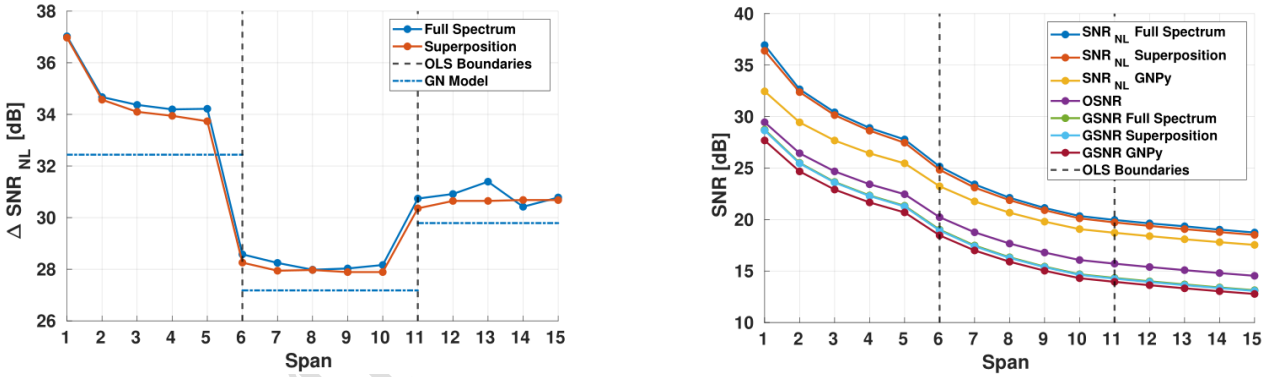

Figure 7: Split-step Fourier method simulation of (a) a full spectrum transmission scenario compared with that of a pump-and-probe superposition, and (b) the SNR_{NL} accumulation along with an OSNR calculated by considering ideal amplification, and the corresponding GSNRs for the full spectrum, superposition and GNPy simulations.

Moreover, in order to evaluate the disaggregation approach in a wideband scenario, the dispersion can be expressed as [18]:

$$\Delta\beta(f, f_1, f_2) = \beta(f_1 + f_2 - f) - \beta(f_1) + \beta(f) - (f_2)$$

and $\beta(f)$ can be approximated by its second and third terms [17]:

$$\beta(f) = \frac{\beta_2}{2}(2\pi f)^2 + \frac{\beta_3}{6}(2\pi f)^3 = 2\pi^2\beta_2 f^2 + \frac{4}{3}\pi^3\beta_3 f^3$$

Following this approach, in Figure 8 we shown the contributions to the total $P_{NLI}^n(f)$ for the *n*th span, with $n = 10$ of periodic SSFM, using an GNPy implementation following all frequency dependent

parameters described in Section 2 and 3 [20]. For these results, the spectral scenario is composed of 64 WDM channels for each band, following a 75 GHz of grid with symbol rate of 64 Gbaud, namely C, L and S_1. The input power for each band is defined following the same approach of [14]. The contribution of each pump-and-probe for the central frequency of each band is computed by:

$$\eta^{n}_{CUT,PUMP} = \frac{P^{n}_{NLI,CUT}}{P_{CUT} \cdot P^{2}_{PUMP}}$$

providing a separate and normalized NLI contribution of each interfering channel, counting also the CUT itself. Figure 8 presents the contribution of each channel using the GGN, which is compared with the contribution computed by the split-step Fourier method for the channels closest to the CUT up to 500 GHz also computing the channels with spacing of 1 and 2 THz. We also plot the extrapolation of those channels, in order to determine the total contribution of this method using the superposition presented in Figure 7. Analysing the contribution, is possible to see that the GGN provides a conservative estimation (higher values) in almost all combinations of channels.

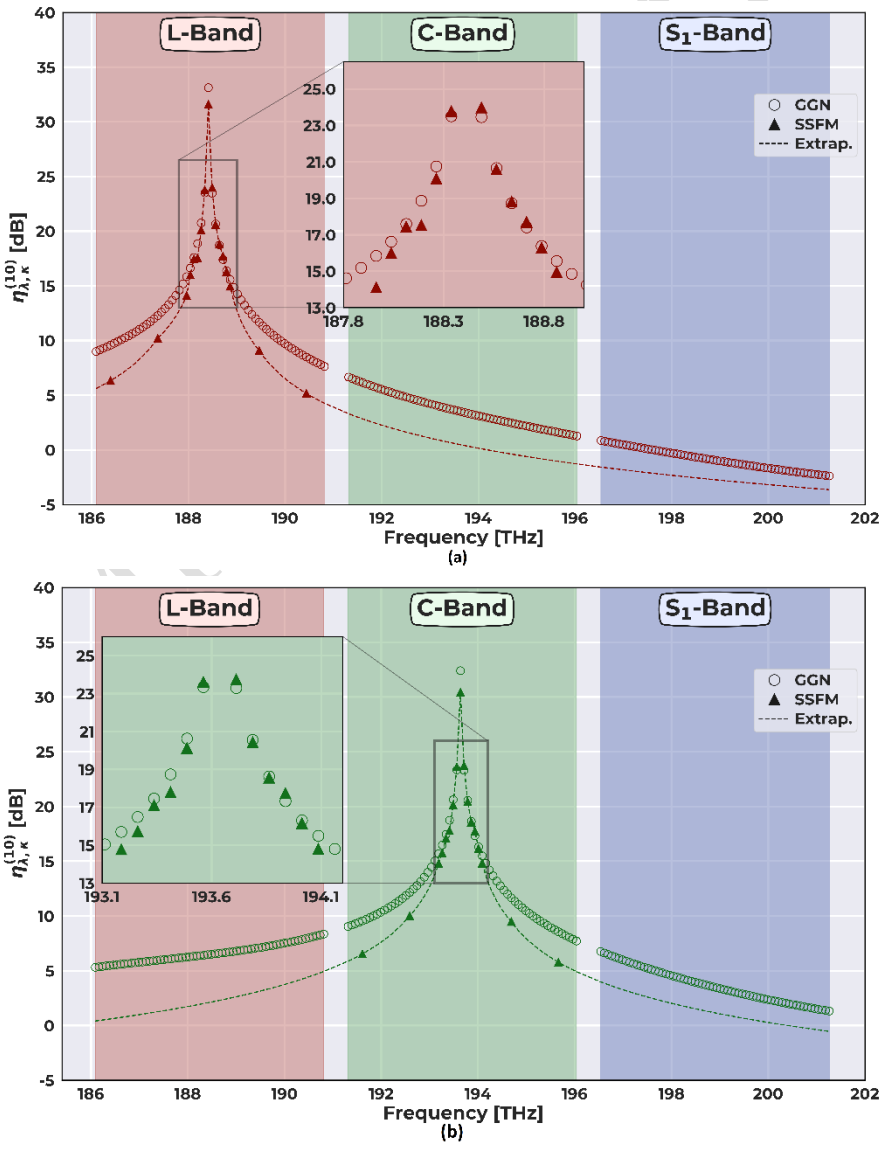

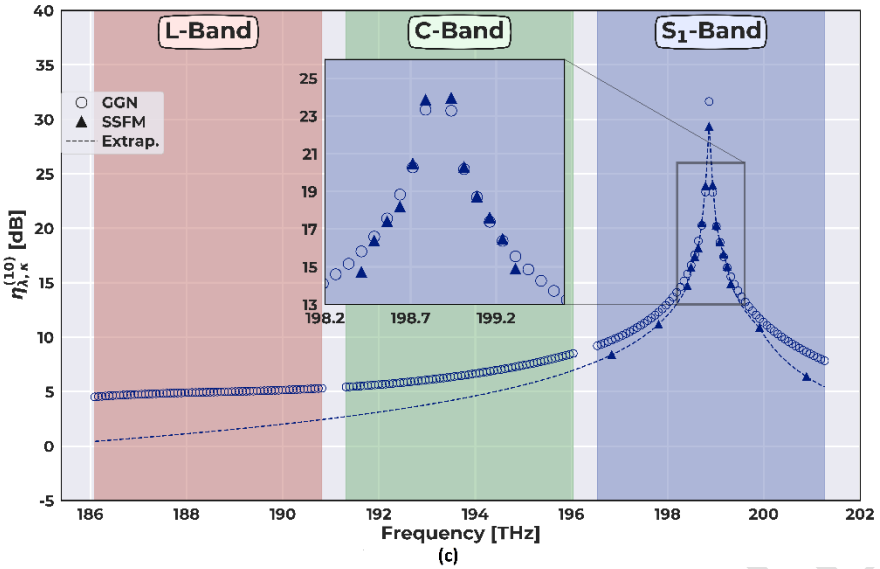

Figure 8: Normalized NLI contribution of all channels (PUMPs) for the central frequency (CUT) of (a) L-band, (b) C-band and (c) S₁-band.

Finally, the SNR_{NL}, the $OSNR$ and $GSNR$ for 7 CUTs in each band are shown in Figure 9, comparing the GGN and SSFM (with extrapolation values to estimate the overall contribution) methods at the end of the 10th span. This limited number of CUTs for each band was chosen due to the SSFM simulation, which requires a significantly computational time to be performed. Moreover, we spread the 7 CUTs along each band, in order to provide a good approximation for all the spectrum used. The SNR_{NL} plots shows that the GGN presents a conservative estimation, with maximum error of 1.7 dB. Regarding the $GSNR$, the conservative aspect is maintained, with maximum error of 0.5 dB. With these results, we show that the GGN method following a disaggregated approach presents a good and conservative estimation of NLI and, consequently, OLS QoT.

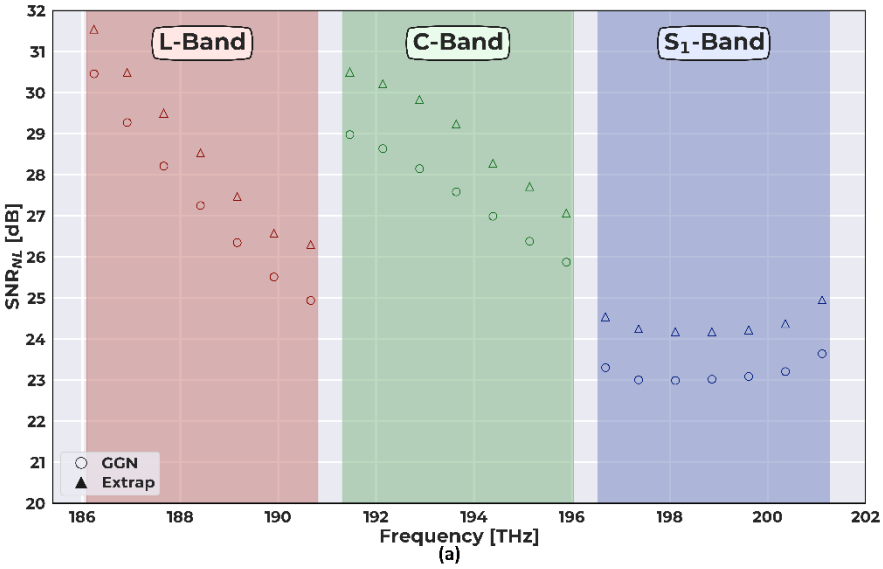

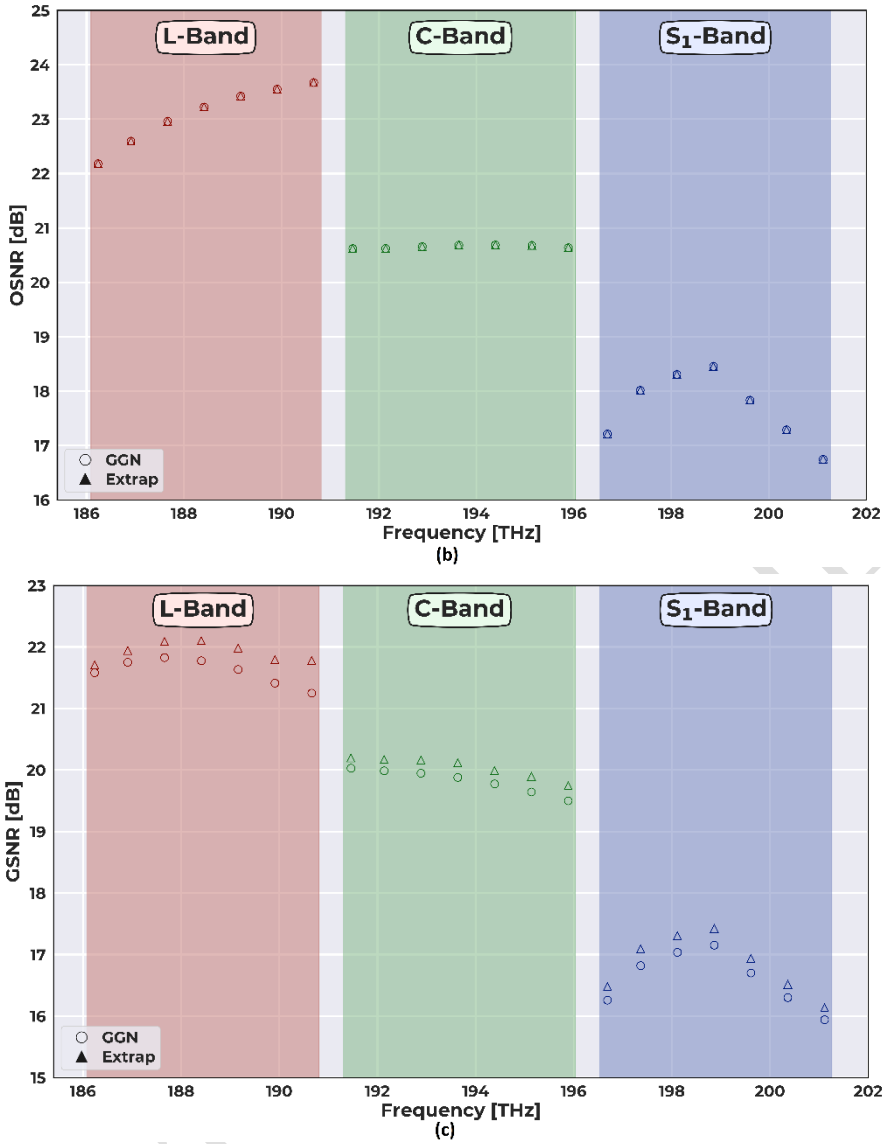

Figure 9: (a) SNR_{NL},(b) OSNR and (c) GSNR plots for 7 CUTs in each band using the GGN and SSFM methods.

4. Conclusions

In this work, we presented several aspects regarding the QoT computation in a disaggregated manner applied in a multi-band context. Firstly, we performed an overview of a multi-band network and its components and modelling assumptions. Secondly, we have shown the characterization of fibre and optical amplifiers required to properly model the QoT computation in a multi-band scenario. Finally, we presented the NLI computation using the GGN model, taking into consideration all the parameters described in Section 2.

We want to highlight that the investigation of the disaggregated method shown in Figure 7 is in the final steps of submission process, already accepted for future publication. Some previous results of this new work are show in Section 3. As soon as this work is published, it can be referenced for better understanding the scenarios and metrics used on it.

5. REFERENCES

[1] A. Napoli, N. Costa, J. K. Fischer, J. Pedro, S. Abrate, N. Calabretta, W. Forysiak, E. Pincemin, J. P.-P. Gimenez, C. Matrakidis, G. Roelkens e V. Curri, "Towards multiband optical systems," em *Advanced Photonics 2018 (BGPP, IPR, NP, NOMA, Sensors, Networks, SPPCom, SOF)*, 2018.

[2] R. Sadeghi, B. Correia, E. Virgilito, E. London, N. Costa, J. Pedro, A. Napoli e V. Curri, "Optimized Translucent S-band Transmission in Multi-Band Optical Networks," em *2021 European Conference on Optical Communication (ECOC)*, 2021.

[3] B. Correia, A. Donodin, R. Sadeghi, V. Dvoyrin, A. Napoli, J. Pedro, N. Costa, W. Forysiak, S. K. Turitsyn e V. Curri, "QoT Evaluation of Optical Line System Transmission with Bismuth-Doped Fibre Amplifiers in the E-Band," em *Asia Communications and Photonics Conference 2021*, 2021.

[4] A. Ferrari, M. Filer, K. Balasubramanian, Y. Yin, E. Le Rouzic, J. Kundrat, G. Grammel, G. Galimberti e V. Curri, "GNPy: an open source application for physical layer aware open optical networks," *Journal of Optical Communications and Networking,* vol. 12, nº 6, pp. C31-C40, 2020.

[5] V. Curri, "Software-Defined WDM Optical Transport in Disaggregated Open Optical Networks," em *2020 22nd International Conference on Transparent Optical Networks (ICTON)*, 2020.

[6] E. London, E. Virgillito, A. D'Amico, A. Napoli e V. Curri, "Observing cross-channel NLI generation in disaggregated optical line systems," em *Asia Communications and Photonics Conference 2021*, 2021.

[7] T. Li, Optical fibre communications: fibre fabrication, Elsevier, 1985.

[8] S. Walker, "Rapid modeling and estimation of total spectral loss in optical fibres," *Journal of Lightwave Technology,* vol. 4, nº 8, pp. 1125-1131, 1986.

[9] G. P. Agrawal, Fibre-Optic Communication Systems, Wiley, 2010.

[10] M. Cantono, D. Pilori, A. Ferrari, C. Catanese, J. Thouras, J.-L. Augé e V. Curri, "On the Interplay of Nonlinear Interference Generation With Stimulated Raman Scattering for QoT Estimation," *Journal of Lightwave Technology,* vol. 36, nº 15, pp. 3131-3141, 2018.

[11] "Amp-fl8221-sb-16 amplifier datasheet from fibrelabs inc.," Fibrelabs inc, [Online]. Available: https://www.fibrelabs.com/bt amp index/s-band-bt-amp.

[12] J. W. Dawson, L. S. Kiani, P. H. Pax, G. S. Allen, D. R. Drachenberg, V. V. Khitrov, D. Chen, N. Schenkel, M. J. Cook, R. P. Crist e M. J. Messerly, "E-band Nd3+ amplifier based on wavelength selection in an all-solid micro-structured fibre," *Opt. Express,* vol. 25, nº 6, pp. 6524--6538, 2017.

[13] A. Donodin, V. Dvoyrin, E. Manuylovich, L. Krzczanowicz, W. Forysiak, M. Melkumov, V. Mashinsky e S. Turitsyn, "Bismuth doped fibre amplifier operating in E- and S- optical bands," *Opt. Mater. Express,* vol. 11, nº 1, pp. 127--135, 2021.

[14] B. Correia, R. Sadeghi, E. Virgillito, A. Napoli, N. Costa, J. Pedro e V. Curri, "Power control strategies and network performance assessment for C+L+S multiband optical transport," *Journal of Optical Communications and Networking,* vol. 13, nº 7, pp. 147-157, 2021.

[15] A. Carena, G. Bosco, V. Curri, Y. Jiang, P. Poggiolini e F. Forghieri, "EGN model of non-linear fibre propagation," *Opt. Express,* vol. 22, nº 13, pp. 16335--16362, 2014.

[16] E. London, E. Virgillito, A. D'Amico, A. Napoli e V. Curri, "Simulative assessment of non-linear interference generation within disaggregated optical line systems," *OSA Continuum,* vol. 3, nº 12, pp. 3378--3389, 2020.

[17] P. Poggiolini, G. Bosco, A. Carena, V. Curri, Y. Jiang e F. Forghieri, "The GN-Model of Fibre Non-Linear Propagation and its Applications," *Journal of Lightwave Technology,* vol. 32, nº 4, pp. 694-721, 2014.

[18] M. Cantono, D. Pilori, A. Ferrari e V. Curri, “Introducing the Generalized GN-model for Nonlinear Interference Generation including space/frequency variations of loss/gain,” ArXiv e-prints, 2017.

[19] A. D’Amico, E. London, E. Virgillito, A. Napoli e V. Curri, “Quality of Transmission Estimation for Planning of Disaggregated Optical Networks,” em *2020 International Conference on Optical Network Design and Modeling (ONDM)*, 2020.

[20] A. D'Amico, B. Correia, E. London, E. Virgillito, G. Borraccini, A. Napoli e V. Curri, “Scalable and Disaggregated GGN Approximation Applied to a C+L+S Optical Network,” *Journal of Lightwave Technology,* 2022.